

Permeability in the thin section

Ayako Kameda
Stanford University, USA
kamedaa@stanford.edu

Jack Dvorkin*
Stanford University and Rock Solid Images, USA
j.dvorkin@rocksolidimages.com

SUMMARY

Numerical simulations of fluid flow through 3D pore space can provide accurate estimations for permeability. A digital volume required for these numerical experiments may be obtained directly by microtomography or statistically reconstructed from 2D thin sections. Such a digital pore volume has to be statistically representative of the original rock. However, only small rock fragments, such as drill cuttings, and only 2D images of those may be available in the field. To address this practical constraint, we investigate how permeability can be estimated from small 2D images. We select a number of natural and artificial medium-to-high porosity well-sorted sandstones. 3D microtomography volumes are obtained from each of these physical samples. Then, analogous to making thin sections of drill cuttings, we select a large number of small 2D slices from a 3D scan. As a result, a single physical sample is used to produce hundreds of virtual-drill-cutting 2D images. Corresponding 3D pore space realizations are statistically generated from these 2D images, fluid flow is simulated in 3D, and the absolute permeability is computed. As expected, this permeability does not match the measured permeability of a physical sample, which is due to inherent variations of pore-space geometry among the small images. However, for all the physical samples, a single and clear trend is formed by cross-plotting the simulated permeability versus porosity. This trend is typical for clean sandstone. The simulated permeability of under-representative sandstone fragments does not match the physically measured data. Instead it provides a valid permeability-porosity transform which can be used to estimate permeability if porosity is independently known from well log or seismic measurement.

Key words: Permeability, Digital, Thin Section.

INTRODUCTION

Numerical experimentation is an attractive complement to physical measurement of rock properties. In such experiments, a physical process is simulated in a pore space and then the corresponding property is calculated. For example, a simulation of viscous fluid flow through pores provides permeability. Many authors have used pore-scale numerical methods, such as Lattice-Boltzmann and network modeling, and showed that absolute and relative permeability can be accurately estimated. Massive and fast numerical experimentation can be used by the geoscientist and engineer in many applications, e.g., to (a) explore the effects of deposition and diagenesis on permeability by digitally altering

the images of original samples; (b) estimate permeability from drill cutting and side-wall plugs which are not large enough for standard laboratory measurements; and (c) relate permeability to other properties, such as electrical conductivity, dielectric permittivity, elastic moduli, and nuclear magnetic resonance (NMR) response.

The necessary input for numerical experiments is a satisfactory digital representation of the pore space in 3D. The 3D image has to be statistically representative of the rock volume. If such images are small, we may expect a significant statistical deviation of the computed porosity and permeability from the "true" physically-measured macroscopic values. There are practical situations where large images are simply not available. Examples are drill cutting, just a few grains across, or damaged rock samples, such as side-wall plugs. Even where large rock images are available, it may be more practical to deal with small sub-samples to speed up the computations and implement a real-time workflow on standard computer hardware. Another practical problem is that obtaining a 3D scan of a rock fragment is still expensive and time-consuming. For example, X-ray tomography of a single sample may take a few hours. On the other hand, preparing a 2D image of a rock fragment is a cheaper and faster alternative to direct 3D scanning and is often done at the drill site.

In light of these practical problems, we will investigate how permeability can be estimated if only 2D images of small fragments of rock are available.

WORKING HYPOTHESIS

It is most certain that the porosity and permeability of the small rock fragments will be statistically scattered around the macroscopic values measured on a large sample. Therefore, it is unlikely that we will be able to obtain this macroscopic permeability from a single small fragment. Instead, we investigate if there is an order in the statistical scatter of the porosity and permeability of the multiple small fragments. We hypothesize that there may be a distinctive trend between the porosity and permeability of the fragments and that once established, this trend can be used to estimate permeability from independent porosity data obtained from well logs or seismic remote sensing.

Our goal is to answer the core question: given that these rock fragments are available and good-quality 2D images of these fragments can be prepared, how do we estimate the macroscopic permeability? To simulate this situation, we select several relatively large high-resolution X-ray tomography 3D scans of natural and artificial sandstone samples. From these scans, we obtain small 2D slices along the plug at even intervals. These slices are intended to represent 2D images of the actual rock fragments available in

the field. From each 2D slice we extract statistical properties which are used in turn to generate a 3D realization of the pore space by pixel-based indicator simulation that uses the porosity and the correlation length of a 2D image. Finally, fluid flow is numerically simulated by the lattice-Boltzmann algorithm to obtain absolute permeability. We analyze the virtual database thus generated.

DATA SET USED

As a test case for our hypothesis, we select a number of medium-to-high porosity clean sandstones. This is the first step toward investigating the applicability of the workflow. We use 3D X-ray microtomography datasets from four natural sandstones, two artificially packed beach sand samples, and a 3D digital description of Finney's sphere pack. The four natural sandstone samples are: Fontainebleau; moderately well-sorted high energy fluvial sandstone from the Hibernia offshore field; two clean aeolian sandstone samples from Wildcat field in Wyoming; and a turbidite sandstone from a North Sea oil field. Two artificially packed samples consist of beach sand from San Gregorio (SG) and Pomponio Beach (PB) from the Northern California coast. The beach sand samples were impregnated with epoxy and then hand-packed in the laboratory. Some of the thin sections are shown in Figure 1.

RESULTS

In Figure 2, we display the computed porosity and permeability for 100 consecutive 2D slices for some of the samples. For each case, including those not displayed in Figure 2, we observe a significant fluctuation of the calculated porosity around the mean value (the latter being very close to the measured porosity). The same is true for the calculated permeability. In general, we expect that the smaller the sample size, the larger the fluctuation.

Let us now cross-plot the computed permeability versus porosity. In Figure 3, these cross-plots are superimposed upon reference data of Fontainebleau sandstone and Ottawa sand. The permeability is normalized by the grain size squared. Figure 3a illustrates our results for the Finney pack. Most of the computed data points deviate from the sample's "true" porosity and permeability shown as a large green symbol. In spite of the strong fluctuation among the computed values, their cross-plot forms a distinctive trend that connects the laboratory Fontainebleau and Ottawa trends. Next, we create three new digital samples by altering the Finney pack. Specifically, we uniformly expand the original Finney pack grains, thus producing lower-porosity samples with macroscopic porosity of 0.258, 0.163 and 0.109. The same procedure is used as with the original Finney pack. The resulting permeability-porosity trends are shown in Figure 3a in orange, brown, and yellow, respectively. All these data still form a tight trend that continues the one observed on the original Finney pack into the lower-porosity domain and matches the laboratory Fontainebleau trend. This result is far from trivial because each data point in these trends was calculated from a small under-representative 2D image of the original sample. Next we examine a number of sandstone samples, starting with a turbidite sample from a hydrocarbon producing field in the North Sea (Figure 3b, red symbols). The simulation results are very similar to those shown in Figure 3a. As expected, most of these data points do not

match the sample's "true" porosity and permeability. However, the scatter plot forms a distinctive trend that connects the laboratory Fontainebleau and Ottawa trends. Similar results are reproduced for other sand samples from different depositional environments: fluvial sandstone from Hibernia field (Figure 3c); aeolian sandstones from Wyoming (Figure 3d); and artificially packed beach sands from California (Figure 3e).

The final frame in Figure 3 displays the results for a single medium-porosity (0.15) Fontainebleau sample (Keehm, 2003) that was scanned and digitized. The trend formed by the porosity and permeability computed from small 2D slices of this sample deviates from the laboratory Fontainebleau trend in the low-porosity domain. A similar behavior can be observed in Figure 3d for the lower-porosity aeolian sample. At this point, it is not clear whether the observed deviation is a numerical artifact or a physical phenomenon.

Nevertheless, our results indicate that while the "true" porosity and permeability cannot be reproduced from small, statistically under-representative, 2D images, a valid permeability-porosity trend can still be established. This result has an important practical implication: in medium-to-high porosity well-sorted sandstones, a permeability-porosity trend can be obtained from small rock fragments unsuitable for standard laboratory measurements. Then this trend can be used to assess permeability from porosity which may be independently estimated from log or seismic data.

CONCLUSIONS

Small fragments of medium-to-high porosity sandstones that are not statistically representative of a larger sample cannot be used to numerically calculate the exact porosity and permeability of the sample. Nevertheless, by using a significant number of such small fragments, we can obtain a valid permeability-porosity trend which can be used to estimate the absolute permeability from independent porosity data.

REFERENCES

- Arns, C.H., M.A. Knackstedt, W.V. Pinczewski, and W.B. Lindquist, Accurate estimation of transport properties from microtomographic images, *Geophysical Research Letters*, 28, 17, 3361-3364, 2001.
- Auzerais, F.M., J. Dunsmuir, B.B. Ferreol, N. Martys, J. Olson, T.S. Ramakrishnan, D.H. Rothman, and L.M. Schwartz, Transport in sandstone: A study based on three dimensional microtomography, *Geophys. Res. Letters*, 23, 705-708, 1996.
- Bakke, S., and P. Oren, 3-D pore-scale modelling of sandstones and flow simulations in the pore networks. *SPE Journal*, 2, 136-149, 1997.
- Bosl, W., J. Dvorkin, and A. Nur, A study of porosity and permeability using a lattice Boltzmann simulation, *Geophysical Research Letters*, 25, 1475-1478, 1998.
- Keehm, Y., Computational rock physics: Transport properties in porous media and applications, Ph.D. Dissertation, Stanford University, 2003.

Keehm, Y., T. Mukerji, and A. Nur, Computational rock physics at the pore scale: Transport properties and diagenesis

in realistic pore geometries, *The Leading Edge*, 20, 2, 180, 2001.

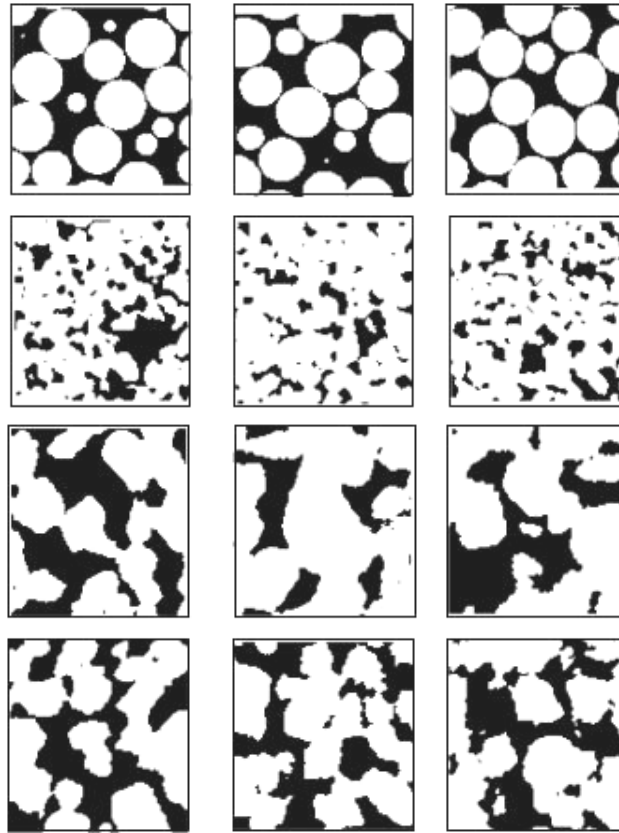


Figure 1: 2D slices of (top to bottom) Finney, Hibernia, Pomponio Beach, and San Gregorio Beach samples.

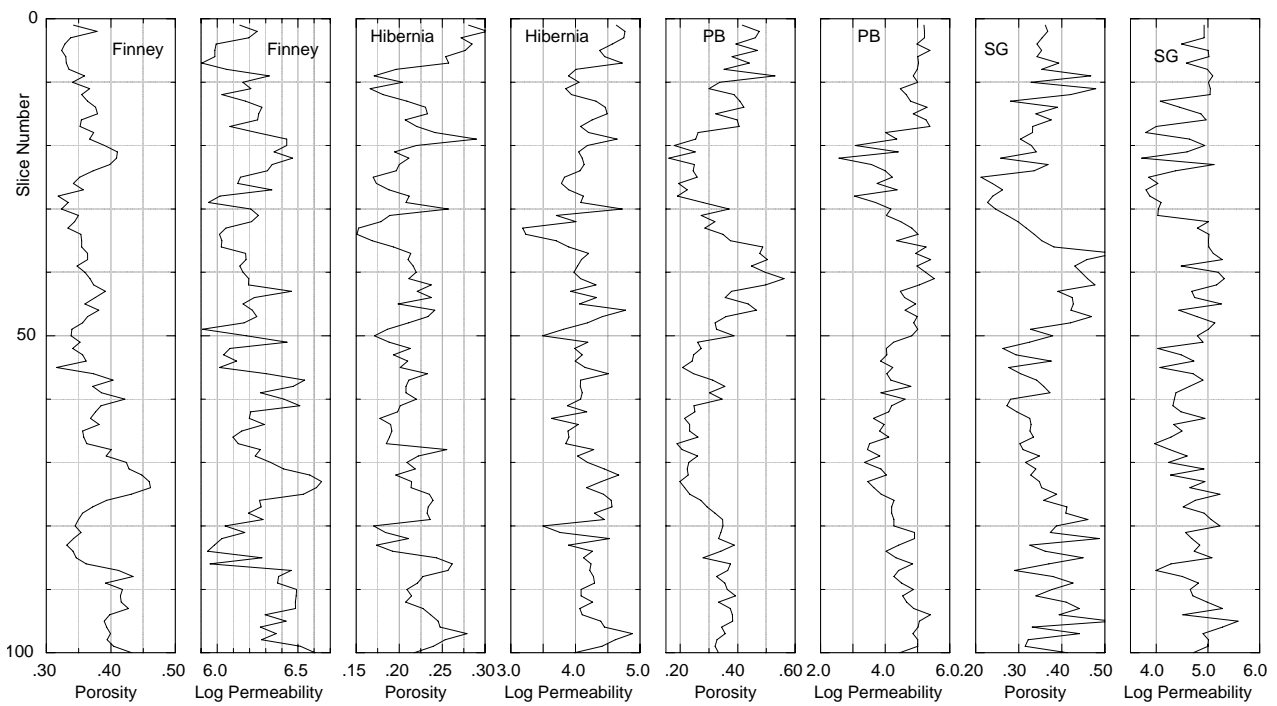


Figure 2: Profiles of porosity and permeability (mD) as calculated from 2D slices for four samples. The vertical axis corresponds to depth along each core and is marked by the slice number. From left to right: Finney, Hibernia, Pomponio Beach, and San Gregorio Beach samples.

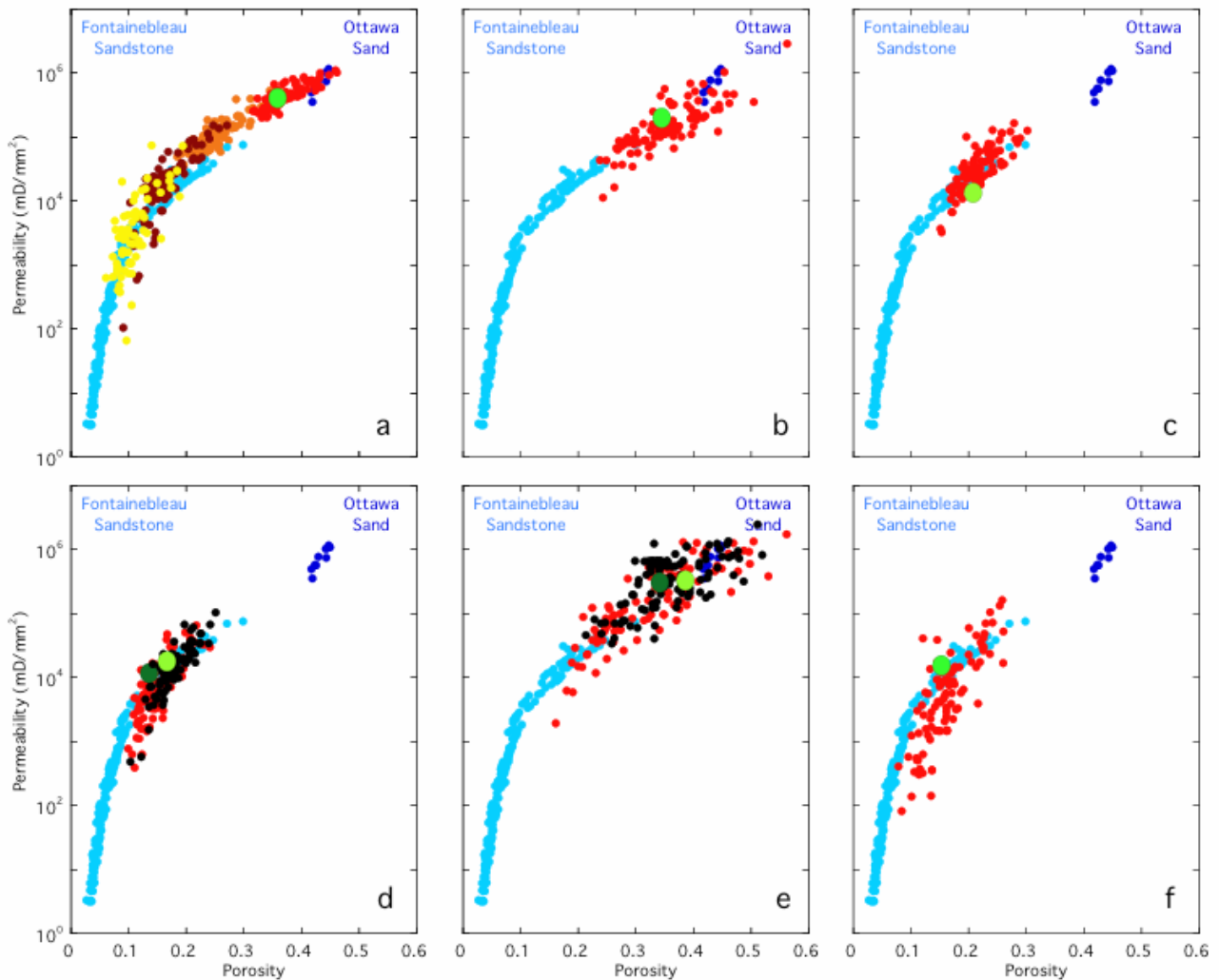


Figure 3: Permeability, normalized by the grain size squared, versus porosity for digital samples under examination. (a) Finney pack (red, orange, brown, and yellow); (b) turbidite sandstone from the North Sea (red); (c) fluvial sandstone from Hibernia field (red); (d) aeolian samples from Wyoming (red and black); (e) artificially packed beach sand samples PB (red) and SG (black); and (f) scanned Fontainebleau sample (red). Large green circles show the measured porosity and permeability for each 3D sample. Where more than two samples are displayed, the tabulated data are shown as dark-green (for red-color trends) and light-green (for black-color trends) symbols. In all frames, laboratory data trends are shown for Fontainebleau sandstone (light-blue) and Ottawa sand (dark-blue).